Crystallization Kinetics of Pure and Fiber-Reinforced Poly(phenylene Sulfide)

C. AUER, G. KALINKA, TH. KRAUSE, and G. HINRICHSEN*

Technical University of Berlin, Institute of Nonmetallic Materials, Polymer Physics, Englische Str. 20, D-10587 Berlin 12, Germany

SYNOPSIS

Isothermal DSC investigations on pure as well as glass, carbon, and aramid fibre-reinforced poly(phenylene sulfide) (PPS) were carried out in order to obtain informations on the crystallization kinetics, that is, the Avrami exponent, constant, half-time of crystallization, and (final) degree of crystallinity. PPS is a typical representative of semicrystalline polymers with a maximum degree of crystallinity of about 60%. The Avrami exponent reaches values from n = 2.1–2.7 depending on fibre type but independent of crystallization temperature. The system aramid fibre/PPS has a much shorter half-time of crystallization than the other three systems that could be attributed to the high nucleation effect of the aramid fibre surface to PPS. As a consequence of the high nuclei density a transcrystalline zone is built up around the aramid fibre. The relatively low value of the Avrami constant was discussed and a computer simulation attempt was made to understand the measured value quantitatively. © 1994 John Wiley & Sons, Inc.

INTRODUCTION

Poly(phenylene sulfide) (PPS) represents a high temperature resistant, semicrystalline thermoplastic polymer with improved mechanical properties that has been mainly used as matrix material for fibre-reinforced composites in recent years. A great number of papers dealing with the physical properties and crystallization behaviour of pure, blended, and reinforced PPS has been published during the last 6 years.[1-14]

The properties of semicrystalline polymers are dependent on their degree of crystallinity as well as on their morphology and crystal structure. Due to the reduced (and sometimes relatively small) percentage of matrix polymer in composites (with a high filling grade) it is assumed that the crystallization behaviour of PPS within a composite shows differences from that of the pure melt.

The aim of this work is the detailed investigation of isothermal crystallization of pure and fibre-reinforced PPS. The isothermal DSC curves are evaluated in the "classical" manner, that is, according to Avrami[15] and Evans[16] a plot of $\log\{\ln[1 - X(t)]\}$ vs. $\log t$ has been made, with $X(t)$ being the degree of (mass) crystallinity at time t. As is well known, the Avrami–Evans theory is subjected to certain restrictions; nevertheless, for a first rough estimation the so-called Avrami exponent (slope of the curve) and Avrami constant (intercept of the curve) are used as in hundreds of publications on the isothermal crystallization of polymers. Perhaps the expression Avrami exponent should be avoided and replaced by crystallization-exponent as has been done in the foregoing publication of the same authors.[17] Following the papers of Jog and Nadkarni[1] and Desio and Rebenfeld[13] DSC investigations were carried out accompanied by light microscopical observations on nucleation and formation of spherulitic entities.

EXPERIMENTAL

Materials

Three different types of PPS were included in the investigations, namely Ryton V 1 (Phillips), fine

* To whom correspondence should be addressed.

Journal of Applied Polymer Science, Vol. 51, 407–413 (1994)
 CCC 0021-8995/94/030407-07

powder, melt viscosity 90 Pa·s; Fortron 0205 T (Hoechst AG), coarse powder, melt viscosity 70 Pa·s; Tedur A 9112185 (Bayer AG), granules, melt viscosity 15 Pa·s. With the fibre-reinforced composites only Ryton was used as matrix material.

For the production of the composites the following fibre types have been chosen: C-fibres, spin-coated, (BASF), Celion HTA7C B 30-500, 12 k, fibre diameter 7 μm; E-glass fibres, spin-coated, (Owens), Ex 5R28, tex 2400, fibre diameter 16 μm; Aramid fibres, spin-coated, (Akzo), Twaron HM, type 1056, tex 805, fibre diameter 12 μm. The composites were produced in the form of endless tapes by the suspended powder impregnation technique of fibre rovings. Details of the suspension impregnation apparatus and production are given in a forthcoming paper.[18] The fibre content of the composites was held constant with 60% by volume.

DSC-Measurements

A modernized Perkin-Elmer DSC 1B in combination with an IBM microcomputer was used. Preliminary investigations proved 16 mg of material as optimum mass. For isothermal crystallization the samples were heated up to 600 K (327°C), that is, at about 40 K above the melting point. The samples were stored at this temperature for 30 s and subsequently cooled down to the crystallization temperature by cold nitrogen gas. The crystallization curves were then recorded dependent on time.

In order to get the Avrami constant and exponent the DSC curves were integrated step-by-step and the so-called Avrami plots $\log\{-\ln[1 - X(t)]\}$ vs. $\log t$ were computed. In some cases the obtained Avrami curves had to be approximated by two straight lines with different slopes, one for the beginning of crystallization and one for the main part of the process. This means that two different values for both the Avrami constant and exponent were obtained. The final part of the crystallization and also the secondary crystallization were not included in the calculation of the Avrami plots.

The absolute values of the degree of crystallinity were calculated using $\Delta H_m = 80$ J/g for the 100% crystalline PPS according to Brady.[19]

Light Microscopy

The microscopical observations were performed with a polarized light microscope (Leitz Ortholux II Pol-MK). The crystallization temperature was kept constant by suitable heating equipment and the thin specimens were placed between two cover glasses. Photographs were taken after the growing spherulites achieved a sufficiently large size.

RESULTS AND DISCUSSION

Melting and Nonisothermal Crystallization

To ascertain the melting and crystallization behaviour of the different PPS types, usual heating and cooling measurements with a temperature rate of 8 K min^{-1} were performed. The results listed in Table I showed small differences in the melting point, but big differences in the crystallization temperature (i.e., the maximum of the DSC cooling curve).

The temperature at which the polymer remains in the molten state and the storage time at this temperature may play an important role in the crystallization behaviour. This effect can be gathered from Figure 1 that shows the DSC crystallization curves of Fortron dependent on the storage time in the melt at 600 K. The crystallization peak shifts to shorter time and lessens its half-width. On the other hand, under the same treatment Tedur shifts the crystallization peak to a longer time and broadens its half-width. This is caused by molecular processes in the melt, like post-polymerization, depolymerization, change of molecular weight distribution, and cross-linking, which have not been dealt with in the frame of the present work. Due to the observation that Ryton has the lowest crystallization temperature and velocity, this polymer was selected for the following investigations.

Isothermal Crystallization of Pure PPS

Isothermal crystallization of Ryton was performed at 502 K in order to observe the values of Avrami

Table I Melting Point T_m, Crystallization Temperature T_c, and Melt Viscosity MV of Different PPS Types

PPS Type	T_m (K)	T_c (K)	MV (Pa·s)
Tedur	554	518	15
Fortron	556	523	70
Ryton	560	495	90

The obtained melting points are in good accordance with reported values (Lopez and Wilkes[12]): The position of the crystallization temperature and interval is dependent on molecular weight,[6] its distribution, and chain linearity or degree of branching.

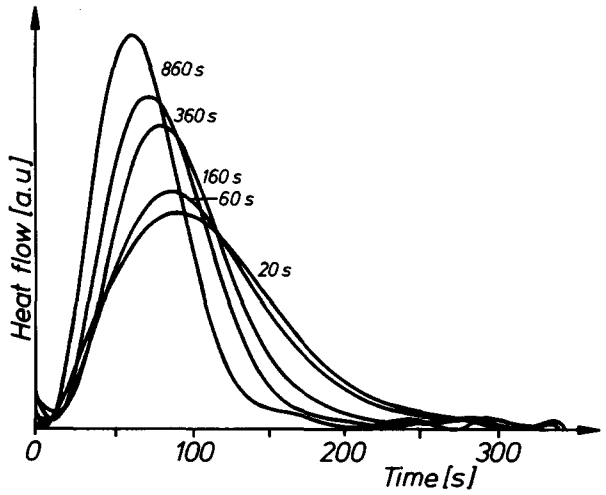

Figure 1 DSC crystallization peaks of Fortron. The storage time in the melt of 600 K was changed.

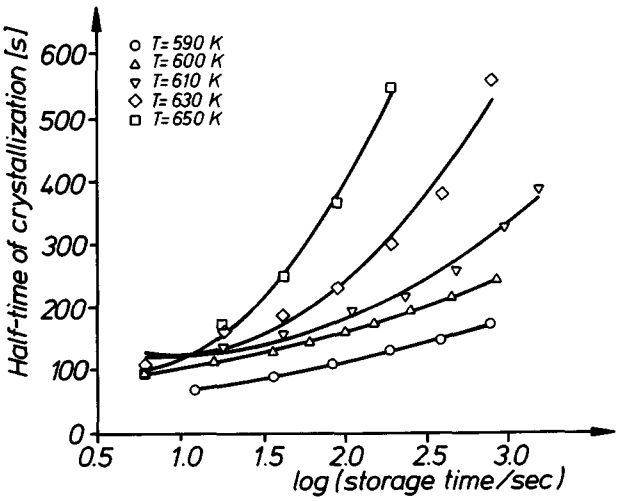

Figure 3 Half-time of crystallization at 502 K dependent on storage time in the melt. Parameter: melt temperature.

exponent n, half-time of crystallization, and enthalpy of crystallization. To get information on the influence of melt temperature and storage time on the crystallization behaviour, four different temperatures were chosen: 590, 610, 630, and 650 K. Figure 2 shows the influence of the melt temperature and storage time on the Avrami exponent n. This quantity appears almost independent of melt temperature, but depends slightly on storage time having values between $n = 2.5$ and $n = 2.1$. This situation changes significantly if the half-time of crystallization comes into consideration (Fig. 3). The half-time depends on both melt temperature and storage time. At the lowest melt temperature (590 K) the half-time increases smoothly with storage time, whereas at the highest melt temperature (650 K) a time factor of 6 is observed. The small half-time values of crystallization at short storage time may be attributed to the fact that remaining parts of crystallites can act as nuclei for the subsequent crystallization. The strong increase of half-time at high melt temperatures may be explained by a molecular cross-linking process.

The chemical alterations are also reflected in the dependence of the specific heat of crystallization on storage time in the melt (Fig. 4). At the lowest melt temperature (590 K) this quantity is nearly independent of storage time, but this enthalpy decreases significantly at the highest melt temperature (650 K). This result proves again that at temperatures

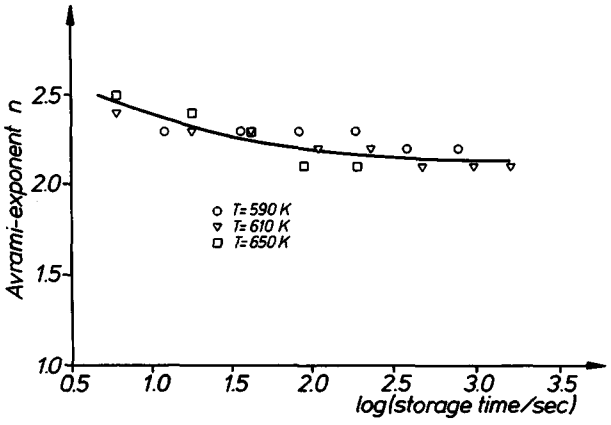

Figure 2 Avrami exponent n at $T_c = 502$ K dependent on storage time in the melt. Parameter: melt temperature.

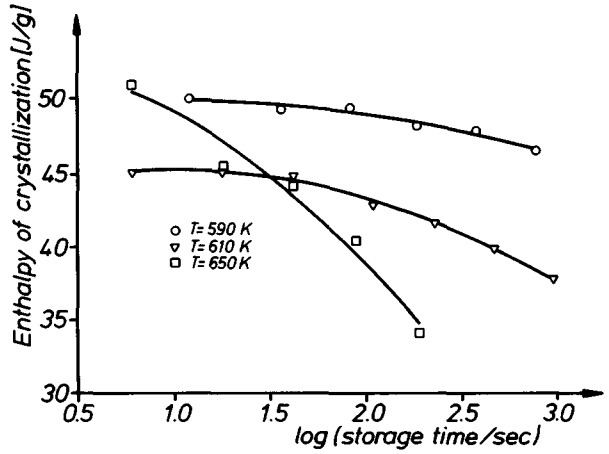

Figure 4 Specific enthalpy of crystallization at 502 K dependent on storage time in the melt. Parameter: melt temperature.

higher than 600 K, PPS undergoes chemical alterations like cross-linking or oxidative damage.

Isothermal Crystallization of Fibre-Reinforced PPS

As mentioned before glass, carbon, and aramid fibres were used as reinforcing materials and a nucleating effect is to be supposed. Figure 5 represents typical DSC curves of isothermal crystallization at given temperature T_c = 502 K. The supposition mentioned above is completely confirmed though in a surprising manner. The crystallization curve of pure PPS takes a medium position and is positioned between the curve of aramid fibre/PPS on the one side and the curves of the C-fibre/PPS and glass fibre/PPS on the other side. The slower crystallization and therefore the lower value of the Avrami constant of the last two systems is connected with the steric hindrance of spherulitic growth of densely filled polymers, as was shown by a computer simulation of crystallization of such systems by Krause et al.[17] On the other hand, the fast crystallization of the aramid fibre/PPS composite proves that the nucleating effect of the fibres is dominant and overcompensates this decrease of dimensionality.[17]

The Avrami plots from the four crystallization curves in Figure 5 contain even more information (Fig. 6). Curves b and d can be represented by just one straight line, that is, one Avrami exponent; the two other curves a and d have to be approximated by two straight lines (one for short and one for longer time, respectively). That means one attains two different Avrami exponents, called n_1 and n_2,

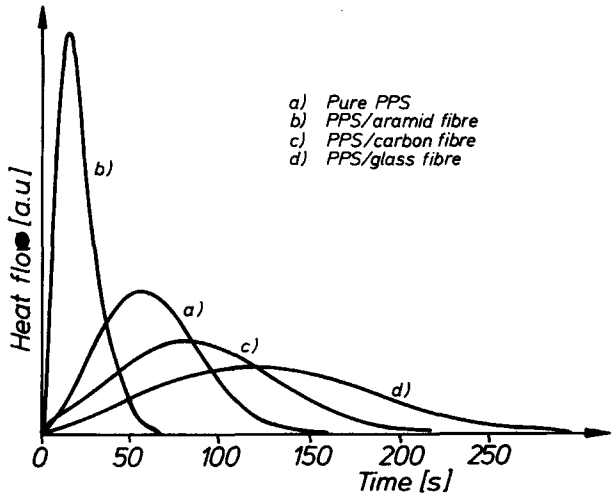

Figure 5 Typical isothermal DSC crystallization curves of pure and fibre-reinforced PPS. Fibre filling grade was held constant at 60% by volume. T_c = 502 K.

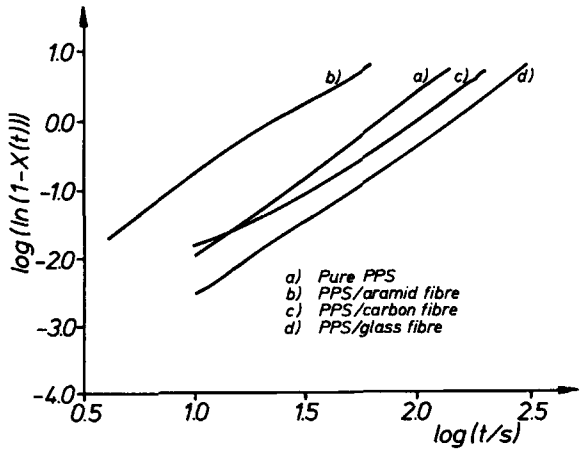

Figure 6 Avrami plots of pure and fibre-reinforced PPS. Specimens and crystallization temperature as in Fig. 5.

respectively. In Figure 7 the obtained Avrami exponents of the different specimens are plotted dependent on the crystallization temperature T_c. It turns out that this quantity differs from sample to sample, but for a given sample it remains constant and is independent of the crystallization temperature. The highest value of n is found for the system aramid fibre/PPS, followed by the pure PPS, and with the lowest values of n by the systems C-fibre/PPS and glass fibre/PPS, respectively. The lowest value of n (1.5–1.7) is attributed to the second part of crystallization of the aramid fibre/PPS, possibly indicating a certain contribution of secondary crystallization. It has to be mentioned that the observable temperature interval of crystallization differs from specimen to specimen. For pure PPS this interval lies between 498 and 513 K, for aramid fibre/

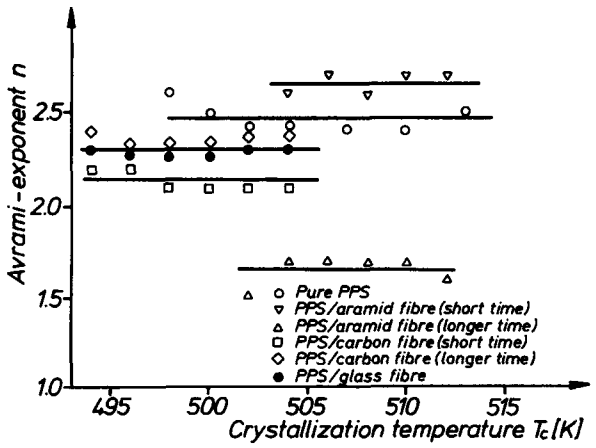

Figure 7 Avrami exponent n of pure and fibre-reinforced PPS dependent on crystallization temperature.

PPS between 502 and 512 K, and for C-fibre/PPS between 494 and 504 K. It can be subsummarized that the Avrami exponents of PPS take up relatively low values (n = 2.1–2.7) as compared to many other crystallizing polymers (n = 2.8–3.4). The reasons for this behavior will be discussed later.

More detailed information can be obtained from knowledge of the Avrami constant k, which is plotted in Figure 8 as a function of crystallization temperature. According to the theory this constant is connected with the radial growth velocity of the spherulites as well as with the number of nuclei. The constant k is expected to decrease with increasing crystallization temperature, a prediction confirmed also for PPS by the results presented in Figure 8. Moreover, there is a great difference between the absolute values of k of the system aramid fibres/PPS and the other three systems. As will be proven in the subsequent section by light microscopical observations, the high values of the constant k for the aramid fibre/PPS composite are due to significant surface induced crystallization by the aramide fibres leading to the so-called phenomenon of transcrystallization.

An additional characterization of the crystallization process is given by the measurement of the half-time of crystallization. From Figure 9 it can clearly be seen that this quantity grows with increasing crystallization temperature. Furthermore, there exists a shift of the corresponding curves in Figure 9 from the system glass fibre/PPS via the systems C-fibre/PPS and pure PPS to the system aramid fibre/PPS. The aramid fibre/PPS composite has by far the shortest half-time values of crystallization.

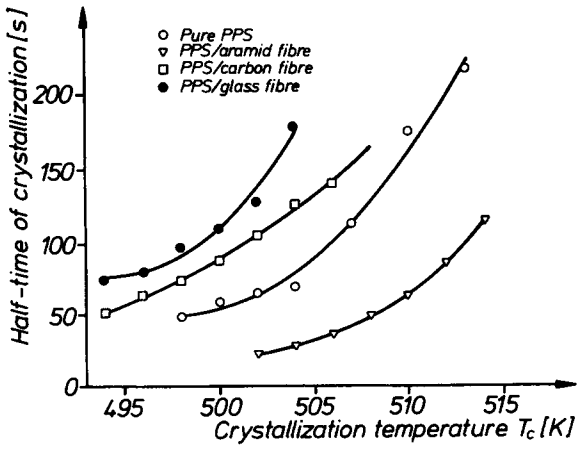

Figure 9 Half-time of crystallization of pure and fibre-reinforced PPS dependent on crystallization temperature.

Figure 10 shows the influence of the crystallization temperature on this characteristic quantity. The enthalpy of crystallization was obtained by the overall integration of the isothermal DSC crystallization curve at given crystallization temperature T_c. The degree of crystallinity was then calculated by putting the measured enthalpy of crystallization into relation to the enthalpy of 100% crystalline PPS. Figure 10 proves that in the case of all investigated PPS systems the degree of crystallinity increases with crystallization temperature and seems to reach an upper limit of 60%. There is only a temperature shift in the curves of Figure 10 indicating again the differences between the system aramid fibre/PPS and the other three systems. The presented results are in good agreement with the results of Desio and Rebenfeld on fibre-reinforced PPS.[13]

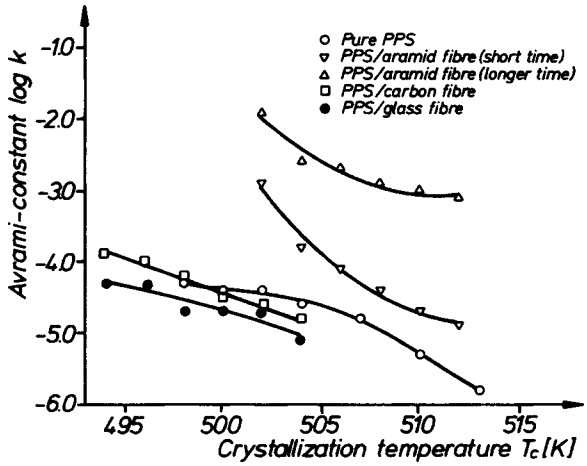

Figure 8 Avrami constant k of pure and fibre-reinforced PPS dependent on crystallization temperature.

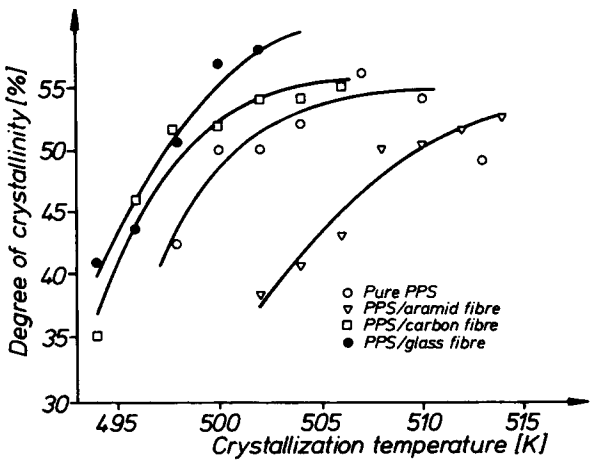

Figure 10 Degree of crystallinity of pure and fibre-reinforced PPS dependent on crystallization temperature.

Light Microscopical Observations

In order to get a better insight into the type of nucleation and the morphology and dimensionality of the crystallizing entities a few preliminary light microscopical investigations have been performed. For this purpose a small number of glass, carbon, or aramid fibres were added to the PPS melt at 610 K. After this, the melt was stored for 30 s and then cooled within the heating and cooling chamber of the microscope down to the crystallization temperature T_c = 494 K. In preliminary experiments this temperature was an optimum for light optical investigations.

Figure 11 represents a compilation of light microscopical photographs of the spherulites within the four investigated PPS systems. The photographs presented here are taken in the final stage of the growth of spherulites. In all cases a spherical morphology is observed, that is, the dimensionality of the growth is equal to 3. As can be clearly seen from Figure 11 (b,d) the glass as well as the C-fibres have no influence on the nucleation and morphology of the spherulites. These pictures differ quite well from that of the aramid fibre/PPS system. The aramid fibres exert a high nucleation effect on the PPS in that a great number of nuclei are formed on the surface of the fibres. The spherulites start crystallizing from the nuclei in a three-dimensional way, but due to the small distance between the neighbouring nuclei the growing entities soon meet and grow in the form of pyramides, discs, or tubes, that is, two- or one-dimensional growth. This process is well-known in many crystallizing polymers and is called transcrystallization.

In the case of fibre/polymer systems with a high filling grade (e.g., 60% by volume or more, which can only be reached with parallelized fibres) one has to consider that the average fibre-to-fibre distance is on the order of ~ 2 μm. This small distance makes the development of a transcrystalline region between the fibres most probable.[17]

It should be mentioned, however, that we succeeded in modifying the surface of the C-fibres, so

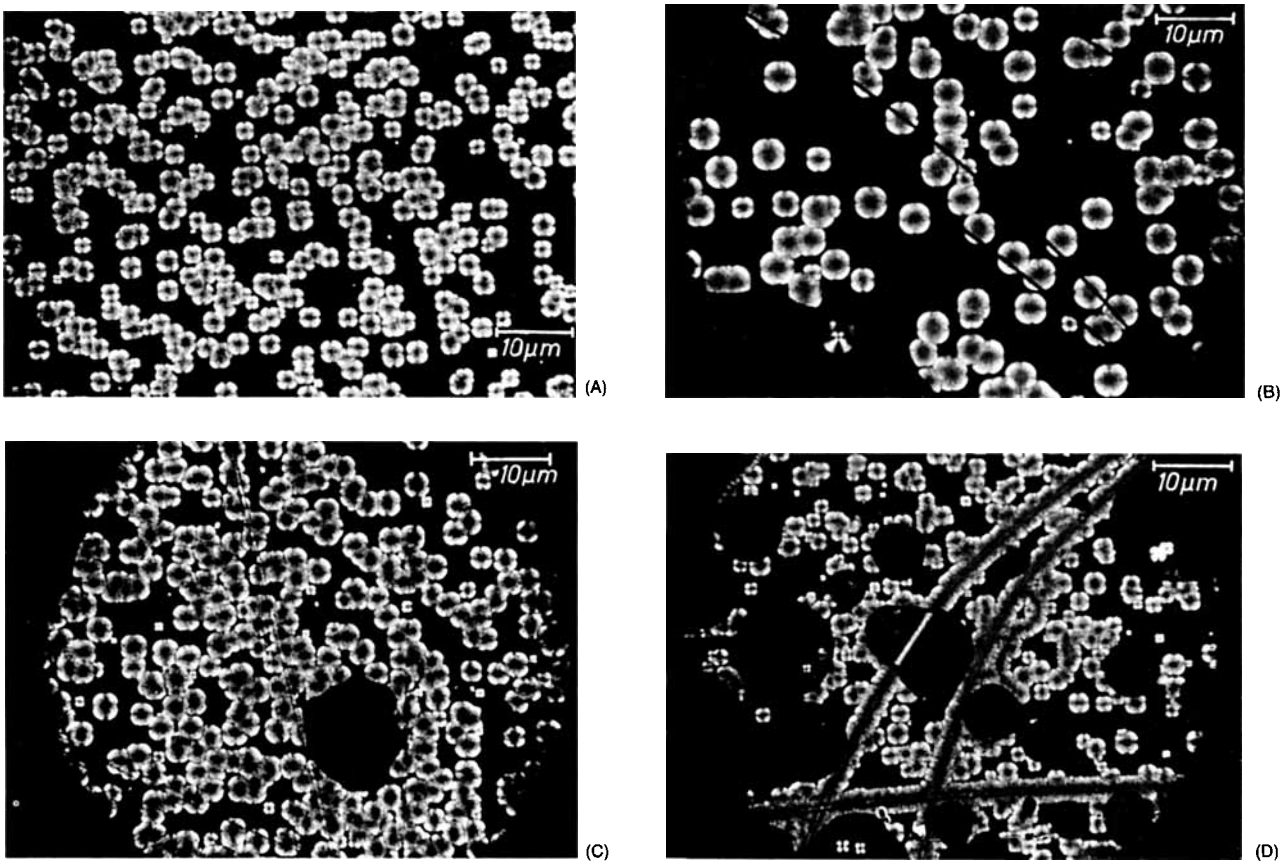

Figure 11 Light microscopical photographs at T_c = 494 K. (a) Pure PPS; (b) glass fibre/PPS; (c) carbon fibre/PPS; (d) aramid fibre/PPS.

that they gave rise to a nucleating effect on PPS. This is preferably done by an electropolymerization of certain monomers on the fibre surface that create a thin overlayer.[20]

Remarks on Crystallization Kinetics

The Avrami–Evans theory[15,16] is well-accepted for the mathematical description of the crystallization of crystallizable polymers. Nevertheless, some restrictions have to be considered; three of them will be discussed in more detail. The first concerns the influence of the secondary crystallization discussed by Dietz.[21] The overall crystallization rate describes the overlapping of the (mostly dominant) primary crystallization and the (mostly subjected) secondary crystallization. In polymers the secondary crystallization starts immediately behind the progressing growth front of the spherulites because of the imperfect phase transition. This overlapping decreases the overall Avrami exponent because the exponent of the secondary crystallization is relatively low. The second restriction deals with geometrical factors. As shown by electron microscopical observations many polymers start their spherulitic crystallization by a rodlike centre and grow via a sheaflike intermediate shape to the well-known spherical form. Calculations in great detail by Dobbert[22] prove that the Avrami exponent depends on the actual shape of the growing spherulite and may vary between 1 and 5. In the case of fibre-reinforced polymers the third restriction plays the most important role as we show in a forthcoming paper.[17] The restriction is due to the limited volume of the crystallizing melt because of the high volume portion occupied by the fibres. Depending on the filling grade, fibre diameter, and average fibre distance as well as on the type of nucleation (homogeneous or heterogeneous) and radial growth velocity, the Avrami exponent takes values from 1 to 4. Generally speaking, the limitations in volume lower the Avrami exponent so that values around $n = 2.3$ observed in this paper can be fully understood.

CONCLUSION

The investigation of crystallization kinetics of (pure and fibre-reinforced) PPS is connected with a great number of influencing factors. From the literature[6] the influence of the molecular weight is known, and in the present paper we have shown that the storage temperature and time of the PPS melt play an important role on crystallization kinetics. Furthermore, the type of reinforcing fibres influences the crystallization behaviour in a substantial manner.

To get even more insight into the complex crystallization behaviour of fibre-reinforced PPS, the fibre content, and consequently the occupied volume and the average fibre-to-fibre distance, will be changed in order to observe its influence on the spherulitic morphology.

REFERENCES

1. J. P. Jog and V. M. Nadkarni, *J. Appl. Polym. Sci.*, **30,** 997 (1985).
2. V. M. Nadkarni and J. P. Jog, *J. Appl. Polym. Sci.*, **32,** 5817 (1986).
3. S. Radhakrishnan and S. G. Joshi, *Eur. Polym. J.*, **23,** 819 (1987).
4. A. J. Lovinger, F. J. Padden, Jr., and D. D. Davis, *Polymer,* **29,** 229 (1988).
5. A. Uemura, M. Tsuji, A. Kawaguchi, and K. Katayama, *J. Mater. Sci.*, **23,** 1506 (1988).
6. J. Koschinski and K. H. Reichert, *Makromol. Chem. Rapid Commun.*, **9,** 291 (1988).
7. V. L. Shingankuli, J. P. Jog, and V. M. Nadkarni, *J. Appl. Polym. Sci.*, **36,** 335 (1988).
8. L. D'Ilavio and A. Piozzi, *J. Mater. Sci. Lett.*, **8,** 157 (1989).
9. L. D'Ilavio, A. Martinelli, and A. Piozzi, *Thermochim. Acta,* **146,** 233 (1990).
10. L. C. Lopez, G. L. Wilkes, and J. F. Geibel, *Polymer,* **30,** 147 (1989).
11. L. C. Lopez and G. L. Wilkes, *Polymer,* **30,** 882 (1989).
12. L. C. Lopez and G. L. Wilkes, *J. Macromol. Sci. Rev.*, **29,** 83 (1989).
13. P. Desio and L. Rebenfeld, *J. Appl. Polym. Sci.*, **39,** 825 (1990).
14. B. Chabert and J. Chauchard, *Ann. Chim. Fr.*, **16,** 173 (1991).
15. M. Avrami, *J. Chem. Phys.*, **9,** 177 (1941).
16. U. R. Evans, *Trans. Faraday Soc.*, **257,** 413 (1981).
17. Th. Krause, G. Kalinka, C. Auer, and G. Hinrichsen, *J. Appl. Polym. Sci.*, to appear.
18. A. M. Vodermayer, Ph.D. thesis, TU Berlin (1992).
19. D. G. Brady, *J. Appl. Polym. Sci.*, **20,** 2541 (1976).
20. L. Kuhnert and K. H. Reichert, private communication.
21. W. Dietz, *Coll. Polym. Sci.*, **259,** 413 (1981).
22. P. Dobbert, *Acta Polym.*, **41,** 9 (1990).

Received March 16, 1992
Accepted June 3, 1993